

Figure 1. A model of TRMM.

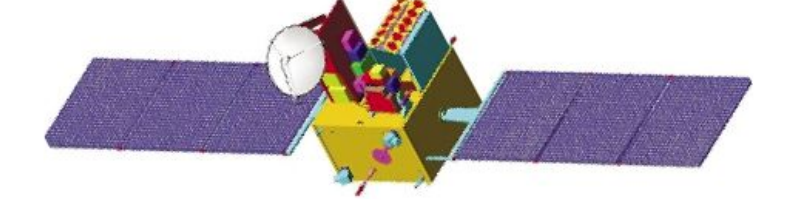


Figure 2. A model of OSCAT.

- | | |
|--|--|
| <p>Tropical Rain Measuring Mission (TRMM) Precipitation Radar (PR) measures rainfall across the globe. Rain rate measurements are considered “truth”.</p> <ul style="list-style-type: none"> Operating Frequency: 13.8 GHz Incidence Angles: range from 0°-20° Swath Width: 150 km | <p>Ocean Scatterometer (OSCAT) measurements of surface backscatter (σ^0).</p> <ul style="list-style-type: none"> Operating Frequency: 13.2 GHz Incidence Angles: 48° and 57° Swath Width: 1400 (inner) and 1836 (outer) (km) |
|--|--|

European Centre for Medium-Range Weather Forecasts (ECMWF): interpolated near-surface wind speed and direction estimates are considered “truth”

Abstract: Ku-band scatterometers were originally designed to measure wind speed and direction over the ocean. Under non-raining conditions the Geophysical Model Function (GMF) captures the relationship between wind speed and direction and sigma-0. However, the presence of rain can distort the observed wind-dependent sigma-0 value, via several effects: (1) Rain drops hitting the surface modify the surface roughness both through splashing and by suppressing the wave spectrum, and (2) falling rain drops attenuate the transmitted and reflected signals and (3) introduce additional backscatter from the drops. Under these circumstances the wind-only GMF accuracy is diminished in predicting the wind speed and direction. Previously, rain specific GMFs have been created for the C-band advanced Scatterometer (ASCAT) (Owen, 2010), and QuikSCAT (Draper and Long 2004; Owen and Long 2011). The Ocean Scatterometer (OSCAT), though similar to QuikSCAT, operated at a different incidence angle and so needs a rain GMF tuned for it.

In order to create a rain GMF for OSCAT, OSCAT sigma-0, Tropical Rain Measuring Mission (TRMM) Precipitation Radar rain, and European Centre for Medium-Range Weather Forecast (ECMWF) surface winds are collocated. TRMM and ECMWF are treated as the “true” rain and wind. Two different rain GMF are made and compared. One for OSCAT sigma-0 standard resolution (L1B) and a second for an Ultra-High Resolution (UHR) sigma-0. BYU UHR algorithm uses reconstruction techniques enhance OSCAT sigma-0 to increase the spatial resolution. The Path Integrated Attenuation (PIA) measurements from TRMM, rain-dependent attenuation and backscatter are combined with the JPL wind GMF to derive the OSCAT rain GMF. The rain GMF is validated using real world data using BYU’s simultaneous wind rain (SWR) algorithm. Wind estimates using SWR under rainy conditions exhibit increased accuracy relative to ECMWF compared with conventional wind-only retrieval (L2B). The results apply to both L1B wind retrieval and UHR wind retrieval.

TRMM and OSCAT Collocation

TRMM operates in a low inclination angle, while OSCAT is in a polar orbit. While this can limit the number of collocations, the TRMM orbit crosses the ASCAT orbit twice per orbit, with many of these within one hour. However for deriving the rain GMF, the temporal difference is limited to 30 mins and the spatial difference is limited to .06 km.

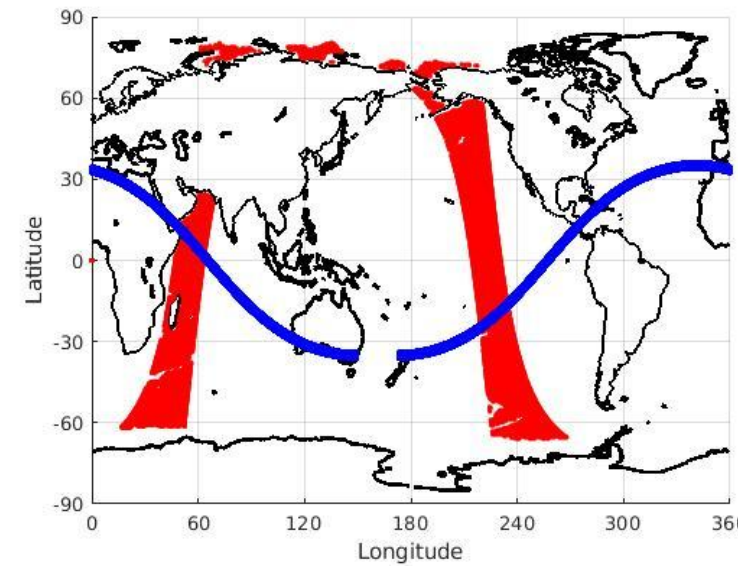


Figure 3. Coverage comparison for corresponding orbits of TRMM (blue) and OSCAT (red).

ECMWF near-surface winds spatially and temporally interpolated to the individual collocation points.

Theoretical Rain Model

$$\sigma^0 = \sigma_{wo}(ws, wd, i) \alpha(R) + \sigma_{eff}(R) + noise$$

σ^0 is the measured backscatter from OSCAT
 σ_{wo} is the no-rain backscatter (i.e., from “background wind”) equivalent to the JPL wind-only GMF which gives sigma-0 as function of wind speed ws , relative wind direction wd , and polarization i
 $\alpha(R)$ is attenuation of the surface sigma-0 due to rain
 $\sigma_{eff}(R)$ is the backscatter resulting from falling rain and surface modification

The rain GMF are the $\alpha(R)$ and $\sigma_{eff}(R)$ functions

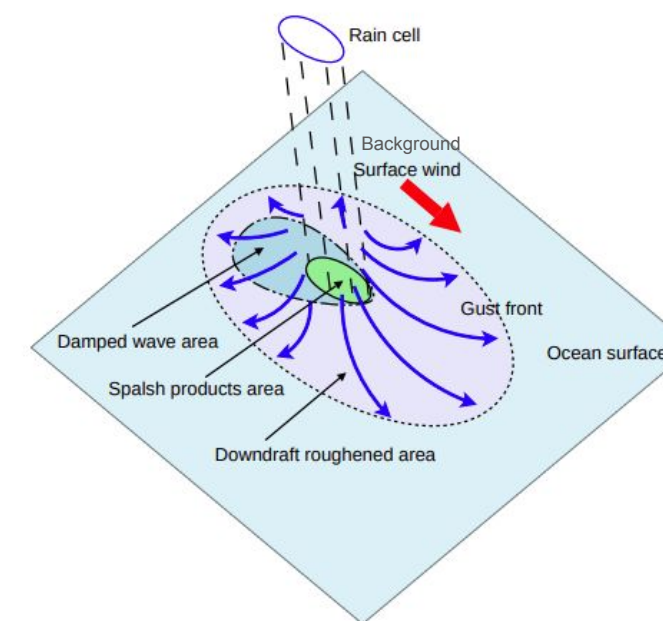


Figure 4. Illustration of how rain cells modify local winds from the “background” large scale wind flow.

The OSCAT Rain GMF (1)

Calculating $\alpha(R)$

$$PIA_{OSCAT} = \cos(\theta_{OSCAT}) / \cos(\theta_{TRMM}) PIA_{TRMM}$$

$$\alpha(R) = 10^{-PIA(R)/10}$$

Fortunately, TRMM measures the Ku-band path attenuated attenuation (PIA), albeit at a different angle than OSCAT. We adjust TRMM PR PIA’s to OSCAT values and fit a non-parametric function to the measurements.

Calculating $\sigma_{eff}(R)$

$$\sigma_{eff}(R) = \sigma_{meas} - \sigma_{wo}(ws, wd, i) \alpha(R) + noise$$

Rearranging the rain model we can solve for $\sigma_{eff}(R)$. Before fitting the data with a non-parametric function, the measured values are binned by rain rate and averaged.

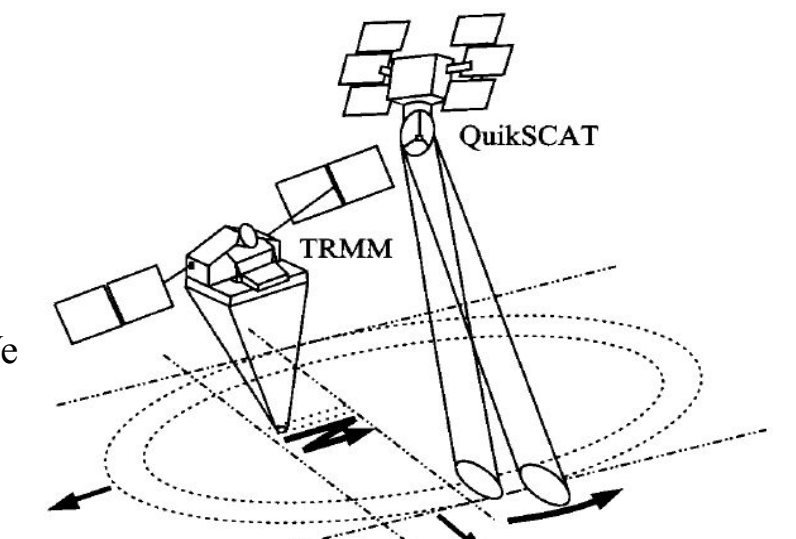


Figure 5. Comparison the swath and scanning of OSCAT and TRMM. OSCAT has two fixed incidence angles (48 and 57 deg), whereas TRMM ranges between 0 and 20 degs on either side of the nadir track.

The OSCAT Rain GMF (2)

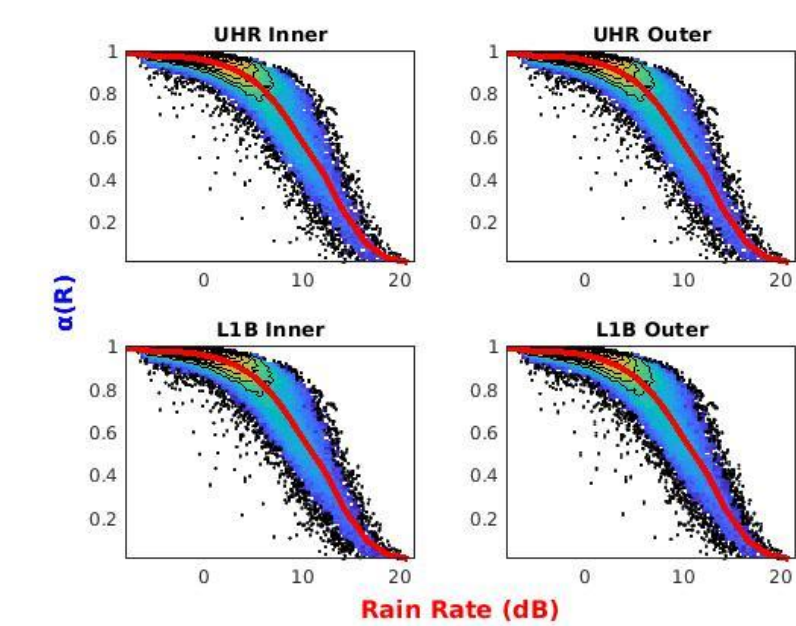


Figure 6. $\alpha(R)$ with respect to rain rate for different incidence angles and measurement resolutions.

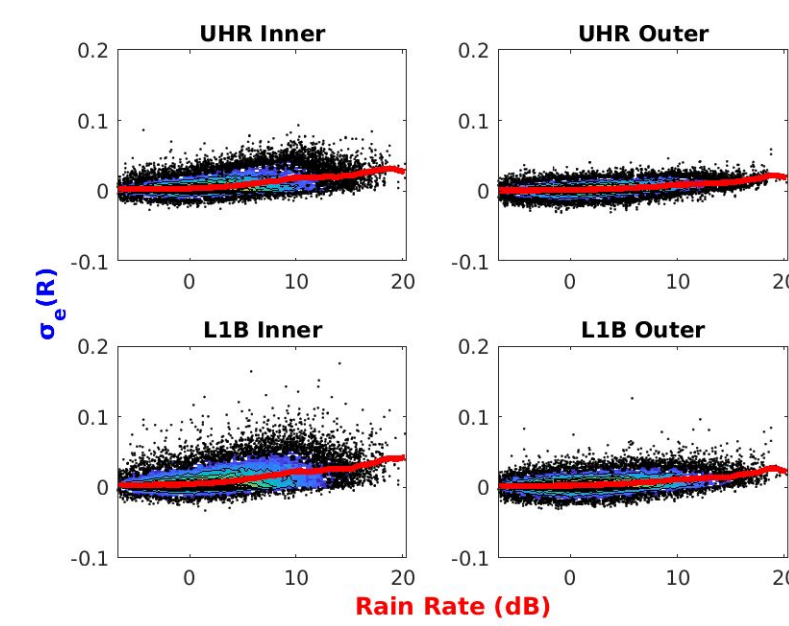


Figure 7. $\sigma_{eff}(R)$ with respect to rain rate for different incidence angles and measurement resolutions.

Simultaneous Wind Rain Retrieval

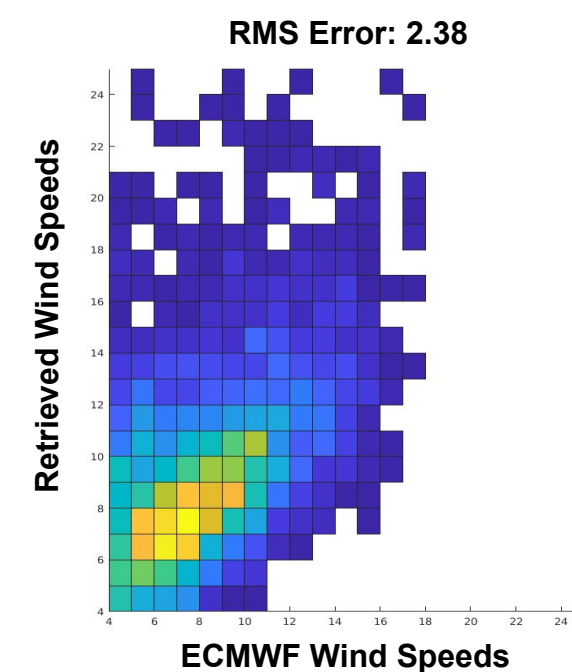


Figure 8. UHR retrieved windspeed using BYU SWR algorithm compared to ECMWF wind speed.

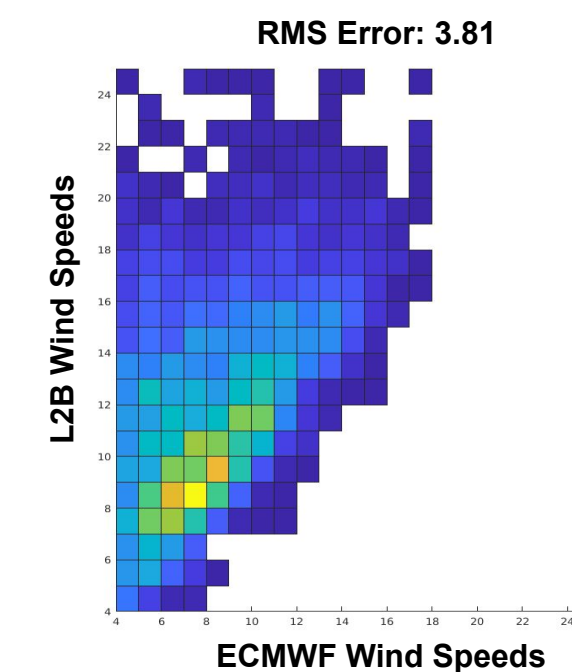


Figure 9. L2B retrieved wind speed using ISRO conventional algorithm compared to ECMWF wind speed.

Bibliography & References

D.W. Draper and D.G. Long, “Evaluating the Effect of Rain on SeaWinds Scatterometer Measurements,” *Journal of Geophysical Research*, Vol. 109, No. C02005, doi:10.1029/2002JC001741, 2004.

D.W. Draper and D.G. Long, “Simultaneous Wind and Rain Retrieval Using SeaWinds Data,” *IEEE Transactions on Geoscience and Remote Sensing*, Vol. 42, No. 7, pp. 1411-1423, doi:10.1109/TGRS.2004.830169, 2004.

C. A. Mears, D. K. Smith, and F. J. Wentz, “Detecting rain with QuikSCAT,” in *Proc. IGARSS, 2000*, pp. 1235–1237.

F. Naderi, M. H. Freilich, and D. G. Long, “Spaceborne Radar Measurement of Wind Velocity Over the Ocean—An Overview of the NSCAT Scatterometer System,” *Proceedings of the IEEE*, pp. 850-866, Vol. 79, No. 6, doi:10.1109/5.90163, 1991.

M.P. Owen and D.G. Long, “Simultaneous wind and rain estimation for QuikSCAT at ultra-high resolution,” *IEEE Transactions on Geoscience and Remote Sensing*, doi:10.1109/TGRS.2010.2102361, Vol. 49, No. 6, pp. 1865-1878, 2011.

M. P. Owen, Signal Scatterometer Contamination Mitigation, Ph.D. Dissertation, Brigham Young University, Provo, Utah, 2010.

L. Ricciardulli & F. Wentz, “A Scatterometer Geophysical Model Function for Climate-Quality Winds: QuikSCAT Ku-2011,” *Journal of Atmospheric and Oceanic Technology*, Vol. 32, No. 150904131243002. doi:10.1175/JTECH-D-15-0008.1, 2015.

F. Ulaby and D.G. Long, *Microwave Radar and Radiometric Remote Sensing*, ISBN: 978-0-472- 11935-6, University of Michigan Press, Ann Arbor, Michigan, 2013.

F.J. Wentz and D.K. Smith, “A model function for the ocean-normalized radar cross section at 14 GHz derived from NSCAT observations,” *Journal of Geophysical Research*, 104 (C5), 11499– 11514, doi:10.1029/98JC02148, 1999.